

Broadening and shift of the magnesium intercombination line and first triplet line due to the presence of the noble gases

Jerry A. Gelbwachs

Chemistry and Physics Laboratory, The Aerospace Corporation (M2/253), P.O. Box 92957, Los Angeles, California 90009

(Received 6 July 1988; revised manuscript received 24 October 1988)

We have employed a two-laser double-resonance method to measure, for the first time, the broadening and shift of the Mg I intercombination line ($3s3p\ ^3P_1-3s^2\ ^1S_0$) and first triplet ($3s4s\ ^3S_1-3s3p\ ^3P_2$) transition due to the presence of helium, neon, argon, krypton, and xenon. Our measurements were performed at pressures below 1 atm. A semiclassical impact theory interpretation of our experimental cross sections provides insight into the nature of the interaction potentials between the two pairs of levels and the noble gases. Our results can be explained in terms of attractive dispersive forces and short-range repulsive forces. A comparison is made between the Mg I broadening and shift cross sections and cross-sectional data of intercombination lines of other alkaline-earth elements and resonance transitions of alkali-metal vapors.

INTRODUCTION

Collisional line broadening and shifting of atomic transitions has been a subject of keen interest to scientists since the beginning of this century.¹ These studies provide insight into the nature of interatomic forces and, hence, they provide an excellent test of theory. Further, broadening and shift coefficients are useful for plasma diagnostics and analysis of emission from stellar atmospheres² and gaseous discharges. Collisional line broadening also provides an optical bandwidth control method for ultra-narrow-band atomic filters.³

An early description of spectral line broadening and shifts was provided by Mitchell and Zemansky¹ in their classic 1934 text. Subsequent excellent reviews include the 1957 article by Chen and Takeo,⁴ a 1980 article by Lewis,⁵ and the 1982 review by Allard and Kielkopf.⁶

Collisional effects involving the Mg atom are of great interest. Of particular interest for line broadening and spectral shift studies are the intercombination line and the first excited triplet level. The latter transition gives rise to the intense b_1 , b_2 , and b_4 Fraunhofer lines⁷ in the solar spectrum near 517 nm. However, we have discovered a dearth of experimental data for these levels. The void, perhaps, is due to the highly forbidden nature of the intercombination line; i.e., $f=4\times 10^{-6}$, which precludes direct measurement by conventional absorption or emission spectroscopy. Broadening of the singlet resonance line of neutral Mg by the noble gases was measured by Zhuvikin *et al.*⁸ while Giles and Lewis⁹ obtained broadening and shift coefficients for the interaction of this line with argon.

Much of the experimental broadening and shift cross sections deduced from measurements of neutral line profiles has been collected by the use of a variety of discharge and shock tube light sources. Grating spectrometers and Fabry-Pérot interferometers provided the spectral analysis resolution. While much excellent work has been performed with these methods, it has been not-

ed⁵ that these techniques suffer from one or more of four major problems: (1) the inability to measure forbidden lines with very small oscillator strengths; (2) the production of ions and electrons that mask neutral atom interactions; (3) operation at high pressure that could permit collision processes involving more than two bodies, thus nullifying the impact approximation; and (4) limited spectroscopic resolution.

We have applied a modified double-resonance technique that uses tunable single-frequency dye lasers to measure the broadening and shifting of the Mg I intercombination line and first excited triplet in the presence of five noble gases. To our knowledge, this is the first report of such measurements. Our two-laser method has enabled acquisition of spectral line profiles of a weak intercombination line, without the production of electrons and ions, at pressures below 1 atm, and with $\pm 10^{-4}\text{-cm}^{-1}$ resolution.

EXPERIMENTAL METHOD

Our experimental approach to the measurement of the linewidth of $3s3p\ ^3P_1-3s^2\ ^1S_0$ intercombination line and the $3s4s\ ^3S_1-3s3p\ ^3P_2$ triplet transition can be best described with the aid of Fig. 1. A partial energy level diagram of the levels of interest is shown in this figure. A single-frequency blue dye laser is tuned to the 457-nm intercombination line. A second single-frequency laser emits radiation at 518 nm that corresponds to the wavelength of the triplet line originating from the $J=2$ level. The lineshape of the intercombination line is recorded by monitoring with a photomultiplier tube the green emission from the $3s4s\ ^3S_1$ level to the metastable level as the blue laser is electronically scanned over the intercombination line. By monitoring the green emission rather than the blue, the problem of detecting the feeble fluorescence is overcome and spectra with excellent signal-to-noise ratios can be acquired. The resolution of the method is determined by the wavelength stability of the

single-frequency ring dye lasers. It is nominally 3 MHz.

It is noted that the lower level ($3s3p\ ^3P_2$) of the green transition does not correspond to the upper level ($3s3p\ ^3P_1$) of the blue transition. Our measurements were performed in this manner to avoid the possibility of coherence effects manifesting themselves in our spectra and complicating their interpretation. Atomic population is transferred between the fine structure metastable triplet by collision processes that serve to destroy the coherence between the radiation fields and the atomic states. Collisional redistribution of population among the various J levels of the metastable triplet proceeds with high efficiency because weak spin-orbit coupling leads to small energy differences compared to kT . The energy separation between the $J=0$ and $J=1$ levels and the $J=1$ and $J=2$ levels is 19.9 and 40.9 cm^{-1} , respectively.

The collisionally broadened linewidth of the triplet line was obtained in a similar fashion. For this case, the blue laser was tuned to the 457-nm intercombination line. The green laser was then scanned over the same

$3s4s\ ^3S_1-3s3p\ ^3P_2$ line and the green emission from the upper level was recorded.

EXPERIMENTAL APPARATUS AND TECHNIQUE

The apparatus used to acquire the line profiles of the Mg intercombination line and triplet lines is schematically shown in Fig. 2. Magnesium vapor was contained in a stainless steel cell that was held at a nominal temperature of 400°C. Six thermocouple thermometers were placed at various points on the outside of the cell. The cell was enveloped in foil for uniform heat distribution and heated by heating tapes wrapped around the foil. Magnesium metal was loaded into a sidearm that could be independently heated. The side arm was held typically at temperatures 30–40 K below the temperature of the cell to prevent deposition of Mg on the cell walls. The cell was attached to a vacuum system incorporating lines through which noble gases at high pressure could be introduced. All measurements were performed at pressures below one atmosphere to ensure that the collisions responsible for the observed line shapes involved only two bodies.

Sapphire viewing ports were incorporated into the vapor cell to allow passage of the laser beams and collection of Mg emission. Optical excitation was provided by two single-frequency ring dye lasers. The bandwidth of each single-frequency dye laser was ~ 3 MHz and they could be electronically scanned continuously over a 20-GHz range. The typical output power of each laser was ~ 50 mW. Blue light was provided by stilbene 3 dye while coumarin 6 dye emitted the green radiation. Beam splitters were arranged to sample the power in each beam (not shown in Fig. 2) and to direct the laser light into a wavelength reference cell. The reference cell contained tellurium vapor at temperatures between 350°C and 400°C and it was used for the shift measurements. Emission from the reference cell was imaged onto a photomultiplier tube. The fiducial Te emission was recorded simultaneously with each scan of the Mg profile.

The laser beams entered the vapor cell from opposite sides and overlapped in the middle. Magnesium emission perpendicular to the direction of the laser beams was collected by a lens and focused onto the photocathode of a photomultiplier tube. A long-wavelength-pass glass filter

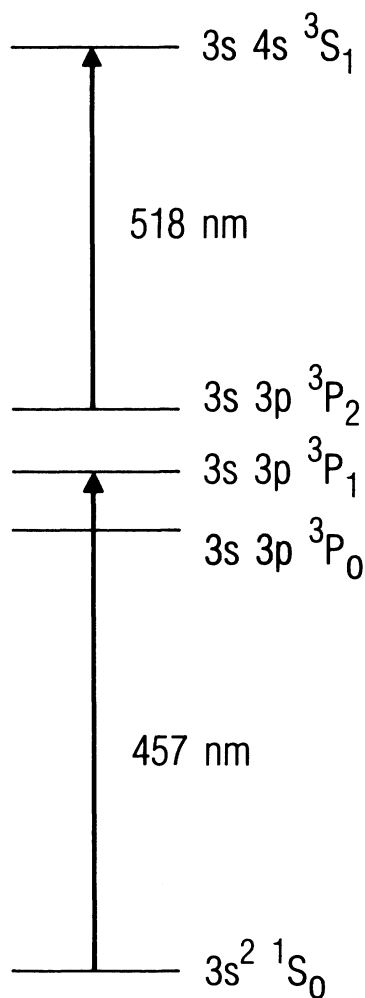


FIG. 1. Partial energy-level diagrams for Mg I. The laser-excited levels are connected with arrows.

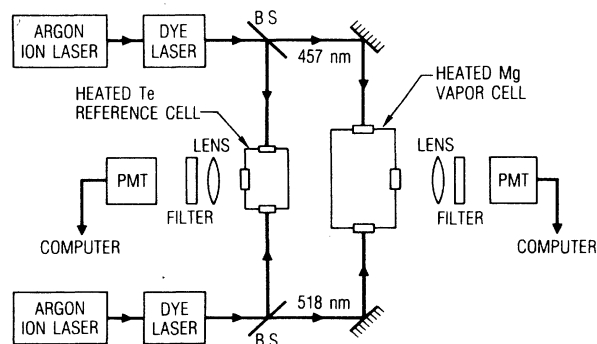


FIG. 2. Schematic representation of the experimental apparatus.

blocked the blue light and allowed transmission of green light. Emission spectra were acquired by fixing the wavelength of one laser while the other was scanned over the appropriate Mg transition. Signals measuring the scanning laser power, the emission from the reference cell, the Mg vapor emission, and the laser scan control were digitized and stored in a laboratory computer. The Mg emission was normalized to incident laser power and printed out together with the reference emission spectrum. The data were also stored on a floppy disk for subsequent processing.

Two examples of data are shown in Figs. 3 and 4. In Figs. 3(a) and 3(b) we display the line shapes of the 518-nm triplet line buffered by 15 Torr and 150 Torr of Xe, respectively. The green emission from the Te reference cell is also shown. Note that the nominal frequencies do not match, owing to variability in the start frequency of the scanning electronics. This figure clearly illustrates the broadening and red shift of the Mg line shape as a function of Xe pressure. In Figs. 4(a) and 4(b), we display analogous experimental spectra for the Mg intercombination line buffered with 10 and 300 Torr of Ar, respectively. For this case, the reference spectrum corresponds to Te emission near 457 nm. Note the excellent signal-to-noise ratio and high resolution of the data in both figures which permitted accurate fits to Gaussian and Voigt profiles.

We recorded asymmetrical intercombination line-

shapes as seen in Fig. 4. The asymmetries were independent of buffer gas and always appeared in the blue wing. A possible source of the asymmetry is the experimental measurement procedure. Measurement sources of line-shape distortion include: nonlinear laser scans, laser beam position drift, power broadening, radiation trapping, long-time constants, and changes in magnesium density during the scan. We exclude measurement factors as the asymmetry source because our recorded 518-nm line shapes, which were obtained using the identical method, exhibited no asymmetry.

Previous laser measurements by Harris *et al.* of the broadening and shift of the calcium resonance line perturbed by the noble gases revealed asymmetric line shapes.¹⁰ They attributed the asymmetry to physical mechanisms associated with the collision process, namely, finite collision time and correlations between pressure broadening and emitter velocity.¹¹ This physical explanation is inconsistent with our data because the noticeable asymmetry manifests itself in the profile of the 457-nm transition only and not on the 518-nm line shape. We do not exclude the possibility of physical mechanisms generating asymmetries in our lineshapes; however, they would necessarily account for only a very small component of the recorded asymmetry.

A more likely explanation for the observed asymmetrical line shape is an isotopic effect. Unlike calcium,¹⁰ in which the major isotope comprises 97% of the natural

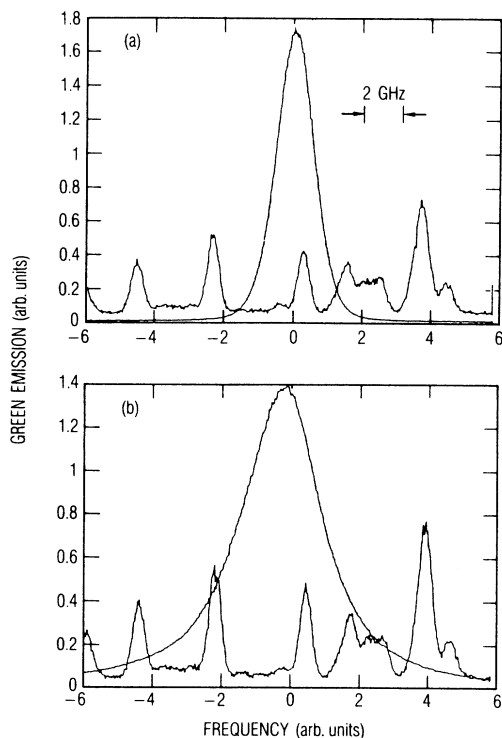


FIG. 3. Emission from the Mg triplet line recorded as the green dye laser scans over the $3s4s\ ^3S_1-3s3p\ ^3P_2$ line. Measurements at (a) 15 Torr (b) 150 Torr of xenon are displayed. A tellurium reference spectrum near 518 nm appears in the lower portion of each plot.

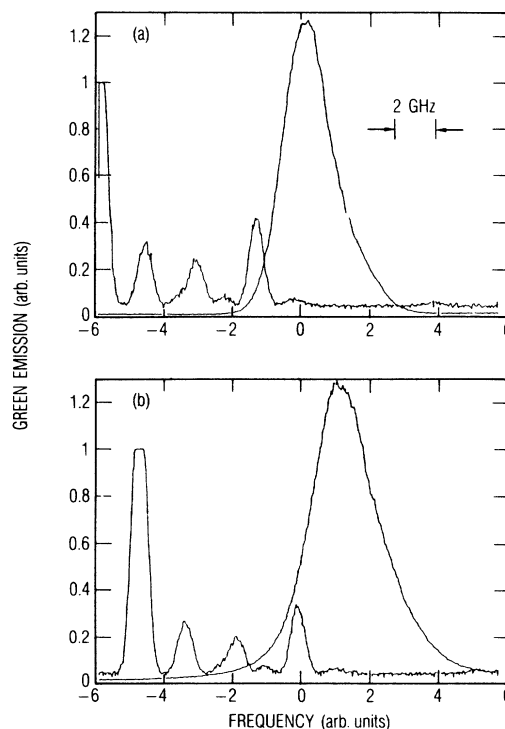


FIG. 4. Emission from the Mg triplet line recorded as the blue dye laser scans over the Mg intercombination line. Measurements at (a) 10 Torr and (b) 300 Torr of argon are displayed. A tellurium reference spectrum near 457 nm appears in the lower portion of each plot.

abundance, the major magnesium isotope, ^{24}Mg , is naturally present at only 79%. The remaining Mg is almost equally distributed among ^{25}Mg and ^{26}Mg . Analysis of the 457-nm line shape in terms of a major isotopic line and a minor line shifted slightly from the center of the ^{24}Mg line shape provides an excellent fit to the data. Also, a shift consistent with isotopic effects, namely, ~ 2 GHz, can be extracted. This analysis is supported by the fact that the measured lineshapes are essentially independent of buffer gas at low pressure. Asymmetry contributed by the mechanism of Harris *et al.* is expected to change with buffer gas species. Further, the isotopic effect explanation is consistent with the lack of asymmetry on the green transition because: (1) the blue laser was tuned to the center of the ^{24}Mg absorption, thus preferentially populating the metastable level with ^{24}Mg atoms, and (2) the isotopic shift associated with high-lying transition tends to be smaller than for transitions involving the ground state.

To obtain the collisional broadening cross sections, we fit the measured line shapes with either a Gaussian profile at pressures below 20 Torr, or a Voigt profile at higher pressures. The asymmetric intercombination line shape was reduced by fitting a Voigt profile centered at the line-shape peak to the red wing of the profile. The residual blue-wing asymmetry was subsequently ignored for linewidth computational purposes. Given the Doppler width, we extracted values for the homogeneous pressure broadening linewidths from our Voigt profiles.

All of our linewidths are full width at half-maximum (FWHM). By dividing these linewidths by pressure, we obtained broadening coefficients. To facilitate comparison with data obtained by other workers as tabulated in the Lewis review article⁵ and to factor out differences in average relative velocities of the different collision partners, we converted our values of pressure broadening coefficients into standard broadening cross sections σ_R . This procedure was followed at each pressure for each of the five noble gases at both 457 and 518 nm.

Our line-shift values were obtained in the following manner: A reference Te emission feature was selected. The frequency difference from this reference line to the center of the Mg line at half maximum was measured from our spectra. This procedure was repeated at each pressure for a given noble gas in one wavelength region. The data were then plotted as line shift (GHz) versus pressure (Torr). A least-squares fit to a straight line was obtained. The slope of the line yielded our shift coefficients. We display our 518-nm shift data in Fig. 5. Similar plots were obtained for the intercombination line. As in the previous case, the experimental shift coefficients were converted into shift cross sections σ_I assuming averages over Maxwellian velocity distributions at 673 K.

To calculate the cross sections from our measured FWHM linewidths $\Delta\bar{\nu}_{1/2}$ and shifts $\Delta\bar{\nu}_0$ both in units of $\text{cm}^{-1}/\text{atom cm}^{-3}$, we used the following expressions:⁵

$$\frac{\Delta\bar{\nu}_{1/2}}{N} = \frac{\sigma_R \bar{v}}{\pi c}, \quad \frac{\Delta\bar{\nu}_0}{N} = \frac{\sigma_I \bar{v}}{2\pi c}$$

where the average relative velocity $\bar{v} = (8KT/\pi\mu)^{1/2}$ and

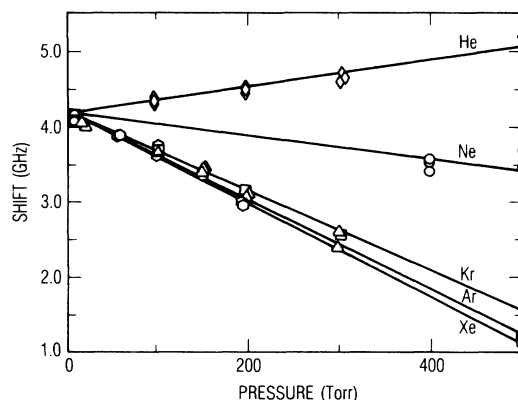


FIG. 5. Line-shift data for the Mg I $3s4s\ ^3S_1-3s3p\ ^3P_2$ line interacting with the noble gases.

μ is the reduced mass of the collision pair.

The Mg triplet lines lie at the short-wavelength edge of the coumarin-6 dye-laser emission curve. Consequently, stable cw operation was most conveniently obtained for the $3s4s\ ^3S_1-3s3p\ ^3P_2$ transition at 518 nm. As a result, we recorded emission spectra primarily on this line. In order to extend our results, we performed several scans over the other members of the triplet. Reproducible, high-quality spectra were obtained. They appeared identical, within experimental uncertainty, to the $3s4s\ ^3S_1-3s3p\ ^3P_2$ line profiles.

We now discuss measurement precision. The major uncertainty in our linewidth measurements originates from the reproducibility of our line shapes. At each pressure, three spectra were recorded. The line shapes were reproducible to within $\pm 5\%$. Each spectrum was computer fit to a Voigt profile. The homogeneous component of the linewidth was then extracted. However, the broadening cross section uncertainty depends upon the relative magnitude of the collisional broadening to the Doppler broadening. Large errors can accrue from small uncertainties in the line shapes at pressures where the collisional broadening is much less than the Doppler width. For most of our cases, the two contributions were comparable in the 200–300-Torr range. Thus, for the 15–500-Torr range of pressures used in our work, Doppler broadening was always a significant component of the linewidth. This fact accounts for the 10–20% uncertainties in our broadening cross-section values.

Our ability to locate the line centers of the Mg profiles and the reference spectral features was the major source of uncertainty in the lineshift measurements. As previously mentioned, we measured the frequency offset from a reference spectrum peak to the center of the full width at half maximum of the Mg line profile in order to determine the collisional-induced lineshift. Figure 5 illustrates this point. When the shifts were small in comparison to the offset, large uncertainties in the slope (shift coefficient) arose. For species with extremely small shift coefficients, such as for the interaction of He and Ne with the intercombination line, measurement uncertainties in the range of 50% accrued. The precision improved to 10% for the noble gases with large shift coefficients.

RESULTS AND DISCUSSION

Our values for collisional broadening (σ_R) and shifting (σ_I) cross sections are displayed in Table I. The broadening cross sections for the intercombination line are the smallest for the lighter noble gases and gradually increase as the noble gas gets heavier. The values range from 70 to 220 \AA^2 . The shift cross sections show more dramatic behavior. The values for He and Ne are very small, namely less than 10 \AA^2 . A tenfold increase in σ_I is observed as one progresses from Ne to Ar. Gently monotonically increasing values for σ_I are recorded for the heavier gases.

Interpretation in terms of interatomic potentials offers a possible explanation of these results. The well-known potential $V(R)$ associated with dispersive forces due to the interaction of two static charge distributions separated by distance R can be expressed as⁶

$$V(R) = -\frac{C_6}{R^6} - \frac{C_8}{R^8} - \frac{C_{10}}{R^{10}},$$

where the C_n 's are coefficients that depend upon the polarizabilities and ionization energies of the collision partners. The first term is the classical van der Waals potential. The second and third terms include higher order polarizabilities that are necessary to accurately describe line-core broadening.

The ratio of broadening to shift cross sections is related to the expression for the dispersive potential by semiclassical collision theory. Values for $2\sigma_R/\sigma_I$ of 2.75, 4.15, and 5.49 have been calculated for long-range attractive dispersive potentials that vary as $-C_6/R^6$, $-C_8/R^8$, and $-C_{10}/R^{10}$, respectively.⁵ In actuality, $2\sigma_R/\sigma_I$ is dependent upon the detailed form of $V(R)$ because the shift arises from the long range component of $V(R)$ while broadening effects occur at short range. However, for the purpose of our analysis we shall use the approximation. Consequently, van der Waals forces shall be presumed responsible for interactions that produce measured $2\sigma_R/\sigma_I$ ratios in the 2.75–5.49 range. Ratios greater than 5.49 and positive (blue-shifted) σ_I values shall be interpreted to signify interactions that are dominated by short-range repulsive forces. The repulsive forces arise from mutual penetration of the electron clouds of the interacting species. A simple closed-form theoretical description of the repulsive force does not exist.⁵

To aid in the discussion of our results we have included the $2\sigma_R/\sigma_I$ ratios in Table I along with the static polar-

izabilities of the noble gases. A dramatic fourfold increase in static dipole polarizability between Ne and Ar is noted. A ninefold gap exists in the quadrupole polarizability values.⁶ These jumps provide a clue to the interpretation of the data.

Let us consider first the 457-nm results. According to semiclassical collision theory the cross section ratios for Ar, Kr, and Xe are consistent with a van der Waals dispersive forces while the σ_R/σ_I ratio for He and Ne reflects a strongly repulsive interaction.

It is noted that the ground-state interaction potential of the Mg-He system has been theoretically calculated.¹² It was shown that the ground level is strongly repulsive with no potential minimum. The minute value of σ_I and its positive sign suggest that the interaction potential of the level derived from the Mg ($3s3p\ ^3P_J$) and He is similar in shape and slightly more repulsive than the Mg-He ground-state potential.

A similar conclusion can be drawn from the Mg-Ne data. The large σ_R/σ_I ratio indicates a repulsive interaction potential. Again, the small magnitude of σ_I suggests parallel potential surfaces. However, because σ_I is negative for this case, the upper level is slightly less repulsive than the ground-state potential.

Thus, repulsive forces account for the interaction of Mg intercombination line with He and Ne. The dramatic increase in shift cross section between Ne and Ar, which coincides with a jump in both the dipole and quadrupole polarizabilities, signals the appearance of a strong long-range attractive potential for the heavier noble gases. These dispersive forces are dominant over the short-range repulsive interaction.

Our cross sections for the triplet transition exhibits a similar pattern. However, compared to the intercombination line, the differences between σ_I for He and Ne and the heavy gases is not as great, and the overall magnitude of the cross sections are 2 to 4 times as large with, of course, the exception of σ_I at 457 nm for He and Ne.

The broadening to shift ratios for Ar, Kr, and Xe are consistent with van der Waals forces acting between Mg and the foreign gas. Once again, the σ_R/σ_I ratio for the lighter gases, He and Ne, suggest that the interaction is dominated by a repulsive force, though one that is weaker than the repulsive force responsible for the interaction with the intercombination line.

Next, it is noted that the magnitudes of the 518-nm cross sections are larger than the 457-nm ones. We offer an intuitive explanation for this result in terms of the po-

TABLE I. Broadening and shift cross sections for the Mg intercombination line and first triplet line.

Noble gas	Relative static polarizability ^a (10^{-24} cm ³)	Mg ($3s3p\ ^3P_1 - 3s^2\ ^1S_0$)			Mg ($3s4s\ ^3S_1 - 3s3p\ ^3P_2$)		
		σ_R (\AA^2)	σ_I (\AA^2)	$2\sigma_R/\sigma_I$	σ_R (\AA^2)	σ_I (\AA^2)	$2\sigma_R/\sigma_I$
He	0.204	70±15	+(3±2)	+46	160±20	+(50±10)	+6.4
Ne	0.395	90±15	-(5±3)	-36	170±20	-(60±10)	-5.7
Ar	1.64	130±20	-(60±15)	-4.3	450±50	-(270±30)	-3.3
Kr	2.48	220±30	-(100±20)	-4.4	450±50	-(260±30)	-3.4
Xe	4.04	200±30	-(100±20)	-4.0	740±70	-(320±30)	-4.6

^aReference 14.

larizability and the atomic radius of the Mg levels. Because of its larger effective principal quantum number, the atomic radius of the $3s4s\ ^3S_1$ level is greater than the radius of the $3s3p\ ^3P_J$. Furthermore, dipole polarizability scales as the square of atomic radius so that the $3s4p\ ^3S_1$ polarizability can be expected to be substantially larger than the $3s3p\ ^3P_J$ polarizability. We now recall that van der Waals interactions exhibit a strong dependence upon the polarizabilities of the atomic levels involved. The repulsive force also depends upon the size of the atom because it originates from the interpenetration of the electron clouds. Thus, for both types of interactions, dispersive or repulsive, the magnitude of cross sections for the triplet line should be greater than the intercombination line values.

Our measurements on the Mg intercombination line can be compared to cross sections for the intercombination line of other alkaline-earth elements such as Cd and Hg.⁵ For Cd, data exist for interactions with He, Ar, and Xe. Our Mg cross sections exhibit similar trends but are overall slightly smaller than the values for the 326-nm Cd intercombination line. Cross sections for the interaction of all five noble gases with the 254-nm Hg intercombination have been measured. Our results for Mg interacting with all five noble gases is very similar, though somewhat smaller, than those obtained for Hg. We note that the broadening to shift ratios for the three heavier noble gases interacting with Hg and Mg all fall within the van der Waals range. They are in close agreement, thus suggesting similar long-range dispersive forces for the two atoms. It is interesting to note that the ratio of oscillator strengths of the three intercombination lines differ by three orders of magnitude. These results can be explained by noting that the alkaline-earth polarizabilities responsible for long range van der Waals forces do not arise from the coupling between the ground and metastable level but originate through the interaction of the ground and metastable levels level with their respective singlet and triplet manifolds.

Our values for the He and Ne shift coefficients for the intercombination line tend to be factors of 2 to 3 times smaller than those measured for Cd and Hg. The corresponding broadening to shift ratios are larger by the same amount reflecting strong repulsive forces. These "hard-sphere" collisions, by their nature, tend to be short range so that it may be reasonable to attribute cross sectional variations in the charge distributions in the immediate vicinity of the respective atoms.

We now discuss our experimental cross sections obtained for the Mg 518-nm triplet transition. O'Neill and Smith¹³ measured the broadening and shift of the Ca I first triplet line due to He, Ne, and Ar at 2000 K. The coefficients of each triplet member was identical to within experimental uncertainty. Because our measurements

were performed at a much lower temperature, we shall not compare σ 's directly. Instead, we compare broadening to shift ratios because of the temperature independence of this ratio according to impact theory.⁵ The two sets of ratios are in close agreement.

Because the 518-nm Mg line is a strongly allowed transition from a metastable level, it would be of interest to compare its broadening and shift cross sections to those values for the first resonance transition of the alkali elements of comparable size. Therefore, we shall perform a comparison with the cross sections for Na and K for which much experimental data exist.⁵ Compared to the Na cross sections, our values appear to be 10–50% higher with the exception of σ_I for He. In this case, σ_I is a factor of 5 larger. Our broadening to shift ratios are in good agreement except for the He case.

Our data is very similar to K cross sections both in the magnitudes of the cross sections and in their ratios with the notable exception, once again, of the He values. For He, the potassium σ_R is 50% larger and σ_I is a factor of 2 to 4 greater than the Mg values.

Therefore, we conclude that dispersive forces are responsible for the long-range interaction of the heavier noble gases with the Mg triplet line in the same fashion as they do with the resonance lines of Na and K. Repulsive forces dominate the interaction with He for all three species. It is suggested that the different He cross sections are due to variations in the charge distributions in the proximity of the atoms, thus giving rise to differing short-range repulsive forces.

CONCLUSIONS

We have measured the broadening and shift of the Mg I intercombination line and first triplet line due to the presence of the noble gases. A two-laser double-resonance technique was employed which yielded excellent high-resolution low-pressure emission spectra. We have calculated broadening and shift cross sections from our measured line profiles. Our data indicate that van der Waals forces are responsible for the interaction of both transitions with Ar, Kr, and Xe. Strong repulsive forces dominate the interactions with He and Ne. Notably small shift cross sections have been recorded for the intercombination line interaction with He and Ne.

ACKNOWLEDGMENTS

The author wishes to acknowledge the help of Dr. H. W. H. Lee in the initial phase of this work, the technical assistance of L. J. Pruitt, and the stimulating discussions with Dr. J. E. Wessel. This work was funded by the Aerospace Sponsored Research Program.

¹A. C. G. Mitchell and M. W. Zemansky, *Resonance Radiation and Excited Atoms* (Cambridge University, Cambridge, 1934).

²A. Unsold, *The New Cosmos* (Springer-Verlag, Berlin, 1977), p. 169.

³J. A. Gelbwachs, *IEEE J. Quant. Electron.* **24**, 1266 (1988).

⁴S. Y. Chen and M. Takeo, *Rev. Mod. Phys.* **29**, 20 (1957).

⁵E. L. Lewis, *Phys. Rep.* **58**, 1 (1980).

⁶N. Allard and J. Kielkopf, *Rev. Mod. Phys.* **54**, 1103 (1982).

- ⁷C. W. Allen, *Astrophysical Quantities* (Athlone, London, 1973), p. 168.
- ⁸G. V. Zhuvikin, N. P. Penkin, and L. N. Shabanova, *Opt. Spectrosc.* **42**, 134 (1977).
- ⁹R. G. Giles and E. L. Lewis, *J. Phys. B* **15**, 2871 (1982).
- ¹⁰M. Harris, E. L. Lewis, D. McHugh, and I. Shannon, *J. Phys. B* **19**, 3207 (1986).
- ¹¹I. Shannon, M. Harris, D. R. McHugh, and E. L. Lewis, *J. Phys. B* **19**, 1409 (1986).
- ¹²C. Bottcher, K. K. Docken, and A. Dalgarno, *J. Phys. B* **8**, 1756 (1975).
- ¹³J. A. O'Neill and G. Smith, *Astron. Astrophys.* **81**, 100 (1980).
- ¹⁴T. M. Miller and B. Bederson, in *Advances in Atomic and Molecular Physics*, edited by D. R. Bates and B. Bederson (Academic, New York, 1977), Vol. 13.